J Math Chem (2015) 53:1733–1749
DOI 10.1007/s10910-015-0515-5

ORIGINAL PAPER

Characterization of conical intersection in a *cis–trans* isomerization through nonclassicality and entanglement

Kinshuk Banerjee[1] · **Gautam Gangopadhyay**[2]

Received: 18 February 2015 / Accepted: 10 May 2015 / Published online: 19 May 2015

Abstract In this paper we have characterized the conical intersection, an important topological feature of potential energy surfaces in a in *cis–trans* isomerization, in terms of the nonclassicality and quantum entanglement which are shown to be controlled by the torsion angle as a molecular parameter. In this context we have provided a quantitative measure of entanglement in terms of Wigner function matrix and compared with other standard measures, namely, von Neumann entropy and partial transpose of joint density matrix. It is shown that the entanglement in the ground state maximizes as the angle reaches the conical intersection point. The highly nonclassical nature of the conical intersection is shown in terms of the significant amount of squeezing for long ranges of the torsion angle and vibronic coupling. The region of high entanglement at and around the conical intersection is connected to the spectroscopically 'dark' time window recently detected in ultrafast transient optical spectroscopy experiments in molecular systems with torsional motion which is associated with the presence of conical intersection.

Keywords Conical intersection · Entanglement · Nonclassicality · *Cis–trans* isomerization

1 Introduction

Investigation and control of the quantum degrees of freedom of a molecule using specially designed femtosecond laser pulses is an area of active research. Quantum

✉ Gautam Gangopadhyay
gautam@bose.res.in

[1] Department of Chemistry, University of Calcutta, 92 A.P.C. Road, Kolkata 700 009, India

[2] S.N. Bose National Centre for Basic Sciences, Block-JD, Sector-III, Salt Lake, Kolkata 700098, India

entanglement and nonclassicality are well studied not only for quantum optical systems but also for molecular and quantum dot material systems. For example, the quantum state reconstruction of a molecule is studied experimentally and from time-dependent spectroscopic analysis of the quantum interference structure due to vibrational motion of a molecule can be completely characterized [1,2]. Generally this characterization involves phase space quasiprobability distributions. Among other measures of nonclassicality and entanglement, von Neumann entropy is utilized to calculate the entanglement of electronic and vibrational degrees of freedom from the joint density matrix. Again the positive partial transpose is applied to composite subsystems which gives a necessary and sufficient condition for separability and entanglement. Among various quasiprobability distributions, Wigner function [3,4] is the most suitable which is extensively used in quantum optics [5] and to exhibit the nonclassicality [6,7] of the electromagnetic field [8–13] and quantum entanglement of the material system [14–17]. Emission tomography was used in the early stages of the quantum state reconstruction of light [8] as well as matter [1,18]. Extensive theoretical and experimental studies were performed on the entanglement of electronic and motional degrees of freedom in trapped atoms and ions [19,20] using the Wigner function matrix concept [21,22]. On the other hand the recent report on the realization of the quantum ground state of a macroscopic mechanical resonator mode and complete quantum control of the mechanical system shows the enormous advance in quantum state realization even for a macroscopic system [23].

Now the effect of quantum entanglement among various degrees of freedom on molecular properties [24,25] is not fully understood due to the added complexity of coupling between the vibrational and electronic motion in comparison to the entanglement between two spatially separated objects. So it is important to study the connection between the entanglement of the system and the way it controls experimentally detectable molecular properties e.g, the spectra and chemical reaction kinetics, in particular. Here we present a study of the nonclassicality and quantum entanglement in the vibrational mode of a molecular system coupled with two electronic states and having also a rotational degree of freedom. This model system exhibits a conical intersection (CI) [26–28] of the two-dimensional adiabatic potential energy surfaces and is well-studied in the context of nonadiabatic ultrafast dynamics of photo-isomerization and internal conversion explained in terms of molecular wavepacket motion [29–32]. The special role of the conical intersection in governing the dynamics of a molecular process particularly for molecules with atomicity greater than 2 is well established [33–35]. In this paper we study the variation of nonclassicality and entanglement over the potential energy surface by treating the torsional coordinate parametrically and characterize the conical intersection point in terms of these quantities. In a *cis–trans* isomerization reaction the torsion angle can be taken as a parameter if a heavy group is attached with the double bond to adiabatically decouple the torsional and vibrational motion. More particularly here it is explored to see how the amount of nonclassicality and entanglement in the ground state depends on the rate of *cis–trans* photoisomerization reaction of the molecular system which is actually governed by the shape of the lower adiabatic potential energy surface [29].

The paper is organized as follows. In Sect. 2 we describe the model system with the Hamiltonian. Section 3 gives the definition and properties of the Wigner

function matrix. Results and discussions are in Sect. 4. The paper is concluded in Sect. 5.

2 A model of conical intersection corresponding to *cis–trans* isomerization

We consider two diabatic [24,31,32] electronic states $|i\rangle$ $(i = 1, 2)$, one being the ground electronic state and the other the first excited singlet state, coupled with a single vibrational mode. Along with this we consider a torsional mode representing the torsion of the molecule around a double bond e.g. the carbon-carbon double bond after electronic excitation. The Hamiltonian of the system is constructed as

$$H = \sum_{i=1}^{2} |i\rangle \left(V_i^t(\phi) + (-\frac{\hbar^2}{2I}\frac{\partial^2}{\partial\phi^2}) + \hbar\omega(a^\dagger a + \frac{1}{2}) \right) \langle i| + \left(|1\rangle\lambda(a^\dagger + a)\langle 2| + h.c. \right). \quad (1)$$

Here $V_i^t(\phi)$ is the torsional potential with ϕ being the torsion angle (coordinate), I is the reduced moment of inertia of torsion; $a^\dagger$, a are creation and annihilation operators, respectively for the vibrational mode with frequency ω and λ is the vibronic coupling constant. The dimensionless normal coordinate of this vibrational mode couples the two diabatic electronic states in first order. The torsional potentials of the two diabatic states are taken from the truncation of the Fourier series as

$$V_1^t(\phi) = \frac{1}{2}v_0[1 - \cos(2\phi)]$$

and

$$V_2^t(\phi) = E - \frac{1}{2}v_0[1 - \cos(2\phi)].$$

We are interested only in exploring the quantum features of the coupling vibrational mode of the system and the characterization of the conical intersection point by treating the torsion angle ϕ parametrically to traverse the lower adiabatic surface. So we choose this simple two-dimensional picture to get an understanding of the connection between the nonclassical features of the states, the vibronic coupling and the role of the topological features like conical intersection of the potential surfaces. In this system the two adiabatic potential energy surfaces exhibit a conical intersection (CI) at $(X = 0, \phi = 48.2°)$ as shown in Fig. 1. For all other values of X and ϕ the degeneracy of PESs is lifted. The dimension of the conical intersection region is zero for the two-dimensional surface [24,25,34] which can be easily visualized and also can be extended easily by including other important degrees of freedom.

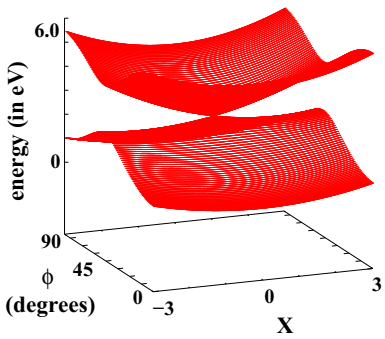

Fig. 1 The adiabatic PESs of the molecular system plotted as a function of the interchain dimensionless normal coordinate X and torsion angle ϕ. A conical intersection is present at $(X = 0, \phi = 48.2°)$

The j-th eigenstate of the molecular system is expanded as,

$$|\psi^j\rangle = \sum_{i=1}^{2}\sum_{n=0}^{\infty} C_{i,n}^{j}|i,n\rangle, \tag{2}$$

where $|i,n\rangle$ is a direct product state with 'n' number of quanta in the vibrational mode. The wavepacket component over the i-th diabatic surface for a given torsion angle is written as [32]

$$\psi_i^j(X) = \sum_{n=0}^{\infty} C_{i,n}^{j}\langle X|n\rangle, \tag{3}$$

where X represents the dimensionless normal mode vibrational coordinate and

$$\langle X|n\rangle = \left(\frac{\sqrt{\omega/\hbar}}{\pi^{1/2}2^n n!}\right)^{1/2} H_n(\sqrt{\omega/\hbar}X)\exp\left(-\omega X^2/2\hbar\right),$$

with H_n being the Hermite polynomial of order n.

3 Measures of entanglement and nonclassicality

3.1 von Neumann entropy

The entanglement between the electronic and vibrational degrees of freedom of the composite states of the system concerned can be expressed using the von Neumann entropy of entanglement [7,36] as

$$E_{\mathrm{VN}} = -Tr_{el}\left(\rho_{el}\log_2\rho_{el}\right) = -\sum_k \gamma_k \log_2 \gamma_k. \tag{4}$$

Here ρ_{el} is the reduced density operator for the electronic degree of freedom (with two-dimensional state space) obtained by taking partial trace over the vibrational degree of freedom of the total density operator ϱ i.e. $\rho_{el} = Tr_{vib}[\varrho]$. γ_k are the eigenvalues

of ρ_{el}. The total density operator ϱ for the j-th eigenstate of the system is constructed from Eq. (2).

Now the von Neumann entropy [37] for the system is defined as $S = -Tr_{el}\,(\rho_{el}\log\rho_{el})$. For unentangled states the entropy is zero and so is E_{VN}. On the other hand, the maximally entangled state with state space of dimensionality D has the maximum entropy $\log D$ [37]. So for the electronic degree of freedom with two electronic states, the maximum entropy will be $\log 2$ and the maximum entanglement will be $E_{\mathrm{VN}} = 1$.

3.2 Positive partial transpose

The positive partial transpose (PPT) [38–40] is a necessary condition for a given joint density matrix of two systems to be separable. It is also known as the Peres–Horodecki criterion. The criterion states that if the joint density matrix ϱ is separable then its partial transpose ϱ^{PT} has non-negative eigenvalues. So if ϱ^{PT} has negative eigenvalues, the corresponding state is nonseparable or entangled. The nonpositivity of the partial transpose is a necessary and sufficient condition of non-separability and entanglement of a composite state in two and three dimensions. For higher dimensions, if the eigenvalues are non-negative then the test is inconclusive.

Now the entanglement E_{NPT} between the electronic and vibrational degrees of freedom in the molecular system is defined as [40]

$$E_{\mathrm{NPT}} = -2\sum_i \gamma_i^- \tag{5}$$

where γ_i^- are the negative eigenvalues of the partial transpose of the joint density matrix ϱ with the partial transpose being taken with respect to the vibrational degree of freedom. The value $E_{\mathrm{NPT}} = 1$ corresponds to a maximally entangled state and for an unentangled state $E_{\mathrm{NPT}} = 0$.

3.3 Wigner function matrix

Wigner function is a phase space quasiprobability distribution [3,4] that gives the complete information about the motional state of the system equivalent to the information contained in the corresponding density operator. Wigner function matrix [21] is the extended form of Wigner function to describe the composite system including the electronic degrees of freedom. It is useful for the complete description of the entangled electronic and vibrational motion [21,22] of the molecular system studied. By appropriate measuring techniques [1,2,18–20] the Wigner function can be an index of quantum interference and one can realize the quantum state of a given system.

The Wigner function matrix for the superposed states of the molecular system can be written as [22]

$$W_{ij}(\beta) = Tr[\varrho A_{ji}\delta(\beta - a)]. \tag{6}$$

Here ϱ is the total density operator describing the electronic and vibrational degrees of freedom. A_{ji} is the electronic flip operator given by $A_{ji} = |j\rangle\langle i|$ that gives rise to transition from state $|i\rangle$ to state $|j\rangle$. β represents the complex phase space amplitude of the vibrational motion defined as $\beta = X + iP$ with X being the dimensionless normal vibrational coordinate and P its conjugate momentum. $\delta(\beta - a)$ is the operator-valued delta function [3] defined as the Fourier transform of the displacement operator $D(\xi) = exp(\xi a^{\dagger} - \xi^* a)$ as,

$$\begin{aligned}\delta(\beta - a) &= \frac{1}{\pi^2}\int d^2\xi\, D(\xi) exp(\beta\xi^* - \beta^*\xi) \\ &= \frac{2}{\pi} D(\beta)(-1)^{a^{\dagger}a} D^{\dagger}(\beta).\end{aligned} \tag{7}$$

The Wigner function matrix is Hermitian. The diagonal matrix elements $W_{ii}(\beta)$ give the Wigner functions corresponding to the diagonal density operator in the electronic state space and gives the occupation probability of the electronic state $|i\rangle$. The Wigner function corresponding to the vibrational degree of freedom can be obtained from the Wigner function matrix by simply taking the trace over the electronic degree of freedom [21] and is given as

$$W(\beta) = \sum_i W_{ii}(\beta). \tag{8}$$

The off-diagonal elements $W_{ij}(\beta)$ give the electronic coherence and information about the entanglement between the electronic and vibrational motions. The negativity of the Wigner function reveals the nonclassicality of the vibrational motion and can also give an idea about the entanglement in the system [6,7]. We define the nonclassicality of a particular eigenstate of the system by a parameter δ defined as the volume of the negative portion of the Wigner function [6] in the phase space of the vibrational motion and it is given by

$$\delta = \int_X \int_P (|W(X, P)| - W(X, P))\, dX dP. \tag{9}$$

For a coherent state, the quantum state considered to be the closest one to a classical state, the parameter $\delta = 0$. But we emphasize here that in specific cases δ can be zero or negligible for highly nonclassical states also. For example, for the highly nonclassical Schrödinger cat states considered by Vogel et al. [21], the diagonal Wigner function matrix elements has no negative portion; hence the Wigner function, determined as the trace of the Wigner function matrix, also will be non-negative over the phase space and the nonclassicality parameter will be zero. In this type of situation the nonclassicality is concealed but the quantum entanglement between the electronic and vibrational degrees of freedom present in the system is a strong indicator of the inherent nonclassical nature of the quantum state. The Wigner function matrix elements $W_{ij}(\beta)$ are useful to detect such kind of entanglement with the fact that the

matrix elements are different for different electronic indices i, j for an entangled state [21,41]. Keeping this in mind, we define the entanglement parameter E_{W} for the states of the molecular system as

$$E_{\mathrm{W}} = \int_X \int_P (|W_{12}| - \sqrt{W_{11} W_{22}}) dX dP. \tag{10}$$

There is a general connection between the nonclassicality and entanglement. A nonclassical state can lead to entanglement in the output states generated by mixing this state with the vacuum state in a suitable experimental setup [10,11] which is not possible with a classical state.

4 Results and discussion

We solve the stationary Schrödinger equation in the direct product basis constructed with the two diabatic electronic states and vibrational states corresponding to the coupling mode. The values of the parameters of the Hamiltonian in Eq. (1) are taken from the work of Seidner et al. [31]. We take $v_0 = 4.5\,\mathrm{eV}$ and $E = 5.0\,\mathrm{eV}$ in the expressions of torsional potentials. The value of the reduced moment of inertia, I is taken in such a way that corresponds to an energy value of 0.01 eV ('$1/I$' has energy units). The frequency of the coupling vibrational mode is $\omega = 0.17$ ev and the vibronic coupling constant λ is varied in the range between ω and 2ω. Consequently the torsional motion becomes slowly varying compared to the vibrational motion to treat it parametrically. We determine the energy values and corresponding eigenvectors treating the torsion angle ϕ parametrically. The wavepacket component $\psi_i^j(\mathrm{X})$ (see Eq. 3) is plotted at different vibronic coupling strengths λ over the lower diabatic surface ($i = 1$) for the lowest energy eigenstate ($j = 1$) with $\phi = 45°$ in Fig. 2. As the torsion angle ϕ approaches the conical intersection (CI) point value $\phi = 48.2°$, the initial Gaussian wavepacket starts to split at $X = 0$. The amount of splitting strongly depends on the coupling strength λ as is evident from Fig. 2. For $\lambda = 2.0$ (scaled with respect to ω), the splitting is complete at and near the conical intersection. For $\lambda = 1.5$ the splitting is partial with the single peaked Gaussian becoming double-peaked but there is no complete separation. Finally for $\lambda = 1.0$ there is no splitting of the wavepacket component over the lower diabatic surface for the ground state of the system. This type of behavior is also obtained from the dynamical studies on the motion of wavepackets over the potential energy surfaces with conical intersection [29,30]. The strong vibronic coupling ($\lambda = 2.0$) expels the wavepacket from the region of large nonadiabatic coupling at the CI point and the motion is adiabatic. Similarly for low coupling ($\lambda = 1.0$), the absence of splitting indicates maximum occupation probability at and near the CI point and hence the motion is diabatic. This behavior is explained through the variation of shapes of the lower adiabatic surface along the X direction, changing from double-well to single-well with decreasing vibronic coupling strength and is well-studied in the literature [32].

Here we study the Wigner function matrix elements $W_{ij}(X, P)$ for the vibrational degree of freedom corresponding to the coupling mode for the lowest energy eigenstate

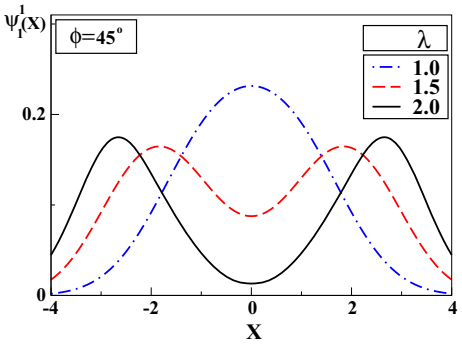

Fig. 2 The wavepacket component $\psi_i^j(\phi, X)$ plotted at different vibronic coupling strengths λ over the lower diabatic surface ($i = 1$) for the lowest energy eigenstate ($j = 1$) with $\phi = 45°$

as a function of the torsion angle ϕ for different values of λ. Different Wigner function matrix elements are plotted over the phase space of the vibrational mode in Fig. 3 for $\phi = 0°$ with $\lambda = 2.0$. The plot of W_{11} corresponds to the vacuum state of vibration and that of W_{22} to the single photon Fock state. The complex off-diagonal element W_{12} contains information about the electronic coherence and entanglement with other degrees of freedom.

The torsion angle ϕ is varied parametrically from 0° to 90° for fixed values of vibronic coupling λ and we study the corresponding variations in the Wigner function elements for the lowest energy eigenstate. The diagonal element $W_{11}(X, P)$ corresponding to the lower diabatic surface is Gaussian-shaped for low ϕ values but starts to split with rising ϕ. The initiation and extent of splitting depends on λ as in the wavepacket picture. For weak coupling ($\lambda = 1.0$) there is hardly any splitting of the element W_{11} over the phase space almost upto the CI point whereas for $\lambda = 2.0$ it starts to split at $\phi \approx 40°$ as in the wavepacket picture. But the Wigner function matrix element exhibits more interesting features. With the generation of two separated peaks over the phase space, there appears a strong interference structure in between. This actually happens for both the diagonal elements W_{11} and W_{22} as the torsion angle approaches the CI point ($\phi = 48.2°$) as shown in Fig. 4. One can see that the two diagonal Wigner function matrix elements corresponding to the two diabatic electronic states has remarkable resemblance with the Wigner functions of Schrödinger cat states [6,42,43], generated by the superposition of two coherent states. In the case of 'cat-states', increasing separation between the superposed coherent states results in the splitting of the initial Gaussian-shaped Wigner function into two lobes with interference structures in between them. In our case both the torsion angle ϕ and the vibronic coupling λ determine the occurrence of splitting and govern the interference structures. For low λ value (say 1.0), the separation and the interference structures are much less pronounced (not shown in figures).

The Wigner function for our system can be calculated from the trace of the Wigner function matrix using $W(X, P) = \sum_i W_{ii}(X, P)$. We have determined the Wigner function for the lowest eigenstate as a function of the torsion angle ϕ and λ. As mentioned in the previous section, the volume of the negative portion of the Wigner function gives a measure of the nonclassicality of the state. We plot the nonclassicality

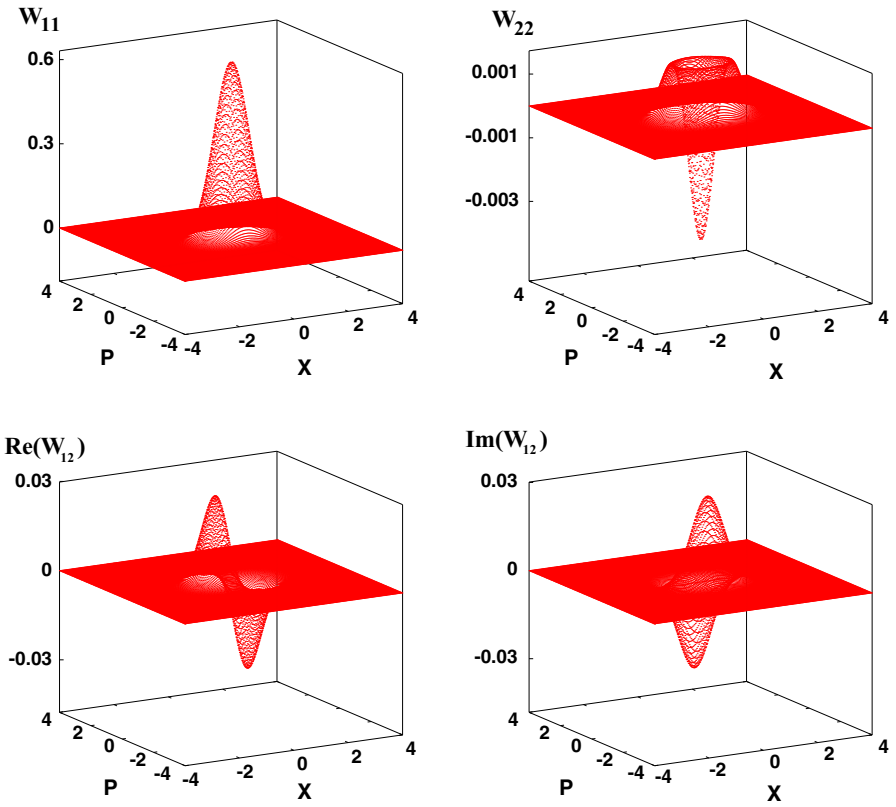

Fig. 3 3D plots of the Wigner function matrix elements W_{11}, W_{22} and real and imaginary parts of W_{12} in the phase space of the vibrational motion for $\phi = 0°$ and $\lambda = 2.0$ for the lowest energy state. X denotes the dimensionless normal coordinate of the vibration and P is its conjugate momentum

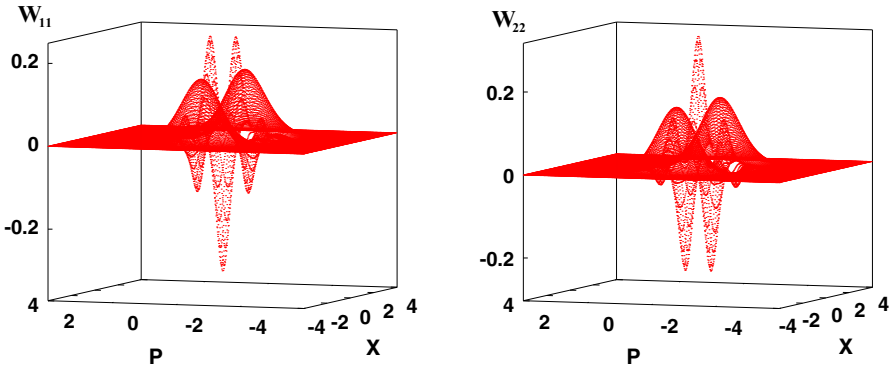

Fig. 4 3D plots of the diagonal Wigner function matrix elements over the phase space of the vibrational motion for the lowest energy state with $\lambda = 2.0$ and $\phi = 48.2°$, the conical intersection point. X denotes the dimensionless normal coordinate of the vibration and P is its conjugate momentum

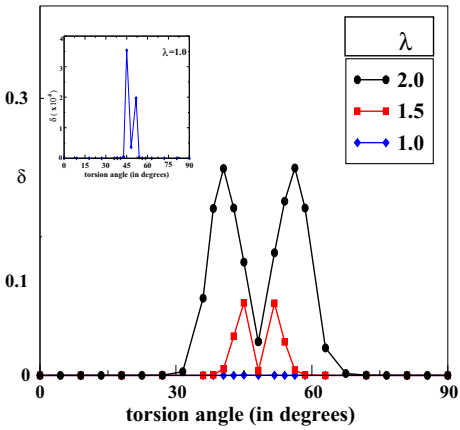

Fig. 5 The nonclassicality indicator δ as a function of the torsion angle ϕ for three different values of the vibronic coupling constant λ for the lowest energy state

indicator, δ, defined in Eq. (9), against ϕ in Fig. 5 for different values of λ. One can see from the plot that δ remains close to zero for ϕ values up to 30° for the range of coupling considered here. In case of strong coupling with $\lambda = 2.0$ the δ value increases sharply for ϕ values greater than 30°. It becomes maximum around $\phi = 40°$ and then decreases almost abruptly and reaches a minimum at the conical intersection point. Beyond the CI point there is a repetition of the features. Similar thing happens for other couplings. We can see that the amount of nonclassicality of the state strongly depends on the coupling strength λ with δ being very small for $\lambda = 1.0$ over the entire range of ϕ studied. But whatever be the value of λ, the nonclassicality indicator δ becomes minimum at the conical intersection point.

From the plots of the diagonal Wigner function matrix elements at the conical intersection in Fig. 4, one can easily see that in this region the interference structures rapidly grow with more pronounced oscillations as the torsion angle reaches the CI point value. These interference structures in the Wigner function matrix occupy a significant negative portion in the phase space and maximize at the CI point. So what is the reason behind the drastic lowering of the nonclassicality indicator δ for the ground state of the system at and near the CI point? With close inspection of the plots of W_{11} and W_{22} in Fig. 4, we can see that their interference structures at the CI point are almost equal in magnitude but of opposite sign over the same phase space region. So when the Wigner function is calculated as the trace over the Wigner function matrix, the interferences of the diagonal Wigner function elements cancel out each other at and near the CI point. That is why the negative volume of the Wigner function and consequently the nonclassicality indicator δ shows a sharp dip at and near the CI point with the value of δ being minimum at the CI point concealing the highly nonclassical feature of the state. The similarity of the lowest eigenstate of our system to the 'cat state' in terms of the diagonal Wigner function elements is already mentioned. The opposite sign of the interference structures for W_{11} and W_{22} extends this link further to even and odd 'cat states' [44]. Hence the lowest eigenstate of the system at the conical intersection point can be described as the superposition of even and odd cat states coupled to the ground and excited diabatic electronic states, respectively and can be written as

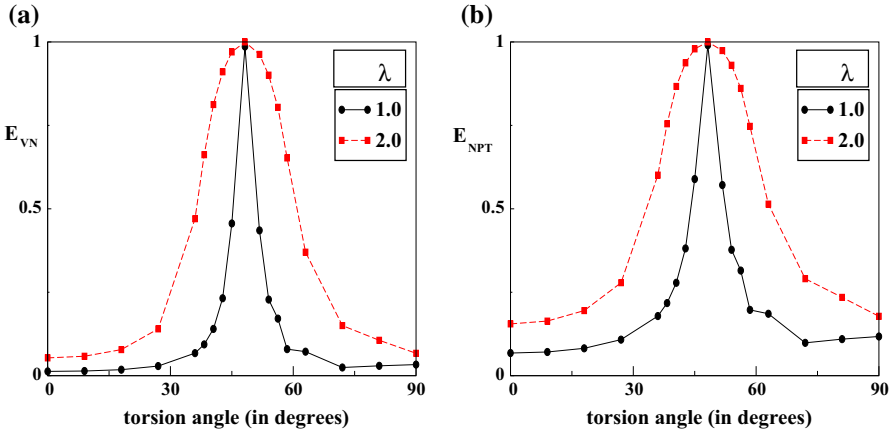

Fig. 6 The entanglement parameters **a** E_{VN} and **b** E_{NPT} as a function of the torsion angle ϕ for two different values of the vibronic coupling constant λ for the lowest energy state

$$|\psi^i\rangle = \frac{1}{\sqrt{2}}\left(|1\rangle(|\alpha\rangle + |-\alpha\rangle) + |2\rangle(|\alpha\rangle - |-\alpha\rangle)\right), \text{for } i = 0. \tag{11}$$

Now to get the actual nonclassical behavior of the lowest eigenstate of the system at and near the conical intersection, we study the amount of entanglement between the electronic and vibrational degrees of freedom for the state. In this context, we have calculated the three different measures of entanglement discussed in the previous section. All the measures are determined for the ground state of the system as a function of the torsion angle parameter ϕ and the vibronic coupling λ. The variations of E_{VN} and E_{NPT} as a function of ϕ for two different values of λ are shown in Fig. 6a, b, respectively. They show almost similar variation trend over the range of ϕ considered for a given λ. With increasing ϕ, at first both E_{VN} and E_{NPT} remain almost constant. Then from $\phi \sim 30°$ there is a sharp rise in both the curves upto the CI point *i.e.* $\phi = 48.2°$. At the CI point both E_{VN} and E_{NPT} become almost equal to their maximum possible value ($= 1.0$) indicating that the ground state of the system becomes a maximally entangled state at the conical intersection point independent of the coupling strength λ. For all other values of ϕ, the two entanglement measures are higher for higher λ. Hence the hidden nonclassical nature of the state at and near the CI point is revealed through the entanglement measures.

Now we introduce another measure of the electron-vibration entanglement, semi-quantitative in nature though, in terms of the Wigner function matrix. An indication of the presence of entanglement in terms of the Wigner function matrix is the fact that for an entangled state the different matrix elements W_{ij} will be different for different electronic indices i, j. So we define an entanglement parameter E_{W} that quantifies the entanglement as defined in Eq. (10). We plot the quantity E_{W} in Fig. 7 as a function of the torsion angle ϕ for two different values of λ for the ground state. From the figure it is seen that the entanglement parameter E_{W} increases with increasing ϕ and its value is higher for higher coupling strength λ. But most importantly E_{W} becomes maximum at the CI point and the actual nonclassical nature of the system gets uncovered. One can

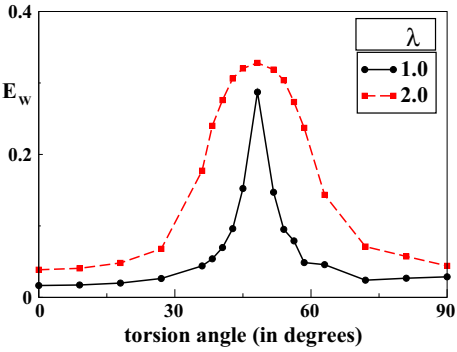

Fig. 7 The entanglement parameter E_W as a function of the torsion angle ϕ for two different values of the vibronic coupling constant λ for the lowest energy state

also see from the figure that the variation of E_W with ϕ shows remarkable semiquantitative similarity with the other two measures of the entanglement (see Fig. 6). This feature can be useful in the context of detection and measurement of entanglement in systems with dimensionality greater than two or three particularly when one must consider the vibrational manifold. Now with the coupled electronic and vibrational degrees of freedom of our system, we can always construct a basis with two pairs of electronic and vibrational states ($|n\rangle = |0\rangle, |1\rangle$) like the problem of two interacting qubits where this choice of basis is the natural one. One point to be noted though is that including only the lowest two vibrational states in the basis is totally justified only when the vibronic coupling is not very strong. But if the quantitative estimation of the entanglement among several degrees of freedom need not be highly accurate without the loss of the general physics then the calculation can be done for strong enough coupling to get an idea about the entanglement variation as a function of relevant system parameters. Then, more importantly, the entanglement variation trend can be matched with the variation of other important and experimentally realizable quantities. This understanding can generate highly interesting informations about the role of the entanglement among several degrees of freedom in governing the properties of the molecular system like current or spectra.

Next we study the variances $\Delta X^2 (= \langle X^2 \rangle - \langle X \rangle^2)$ and $\Delta P^2 (= \langle P^2 \rangle - \langle P \rangle^2)$ as well as the uncertainty product $\Delta X \Delta P$ corresponding to the vibrational mode for the lowest energy state. In Fig. 8 we show the square root of the variances and the uncertainty product as a function of ϕ for two different coupling strengths. From the plots one can see that the uncertainty product $\Delta X \Delta P$ starts to deviate from the minimum uncertainty value of 0.5 as the angle ϕ approaches the conical intersection point. The point at which this deviation commences and also the amount of the deviation depends on the vibronic coupling strength λ. For $\lambda = 1.0$ the deviation starts from $\phi \approx 40^\circ$ whereas for $\lambda = 2.0$ it starts from $\phi \approx 30^\circ$. The deviation of the product $\Delta X \Delta P$ from the value 0.5 becomes maximum at the CI point with its value being higher for higher λ. Also ΔX and ΔP individually become maximum at the CI point which is the point of maximum entanglement as already established for the system concerned. This observation tallies with the study on atom-phonon entanglement [45] where it is established that the uncertainty product for the single particle measurement of a particle's coordinate and momentum is related to the entanglement parameter. These

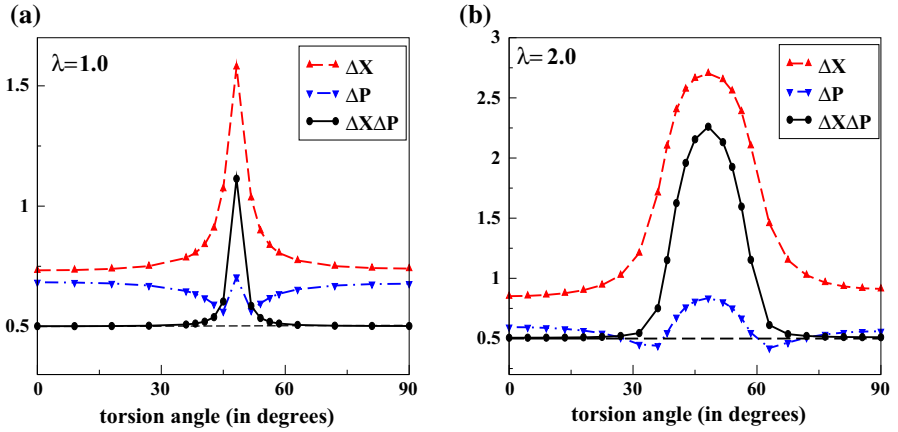

Fig. 8 The square root of the variances, ΔX and ΔP corresponding to the dimensionless normal coordinate X and its conjugate momentum P, respectively for the vibrational mode as a function of the torsion angle ϕ for two different values of the vibronic coupling constant λ for the lowest energy state. The uncertainty product $\Delta X \Delta P$ is shown also

uncertainties, defined individually for the atom and the photon systems, grow with increasing entanglement. The minimum uncertainty product value corresponds to an unentangled state. Another interesting feature is the fact that the variance associated with the P-coordinate, ΔP^2 is less than 0.5 for the case of $\lambda = 1.0$ in the range of ϕ considered and its maximum is at the CI point with the value being very close to but less than 0.5. This is a definite case of squeezing in the P-coordinate. For $\lambda = 2.0$ the squeezing is present upto $\phi \approx 40°$. Above this angle and upto $\phi \approx 55°$ the squeezing vanishes with the value of ΔP^2 being maximum again at the CI point.

The effect of the variations of ΔX and ΔP with the variation of the torsion angle ϕ on the corresponding Wigner function $W(X, P)$ is also very interesting. We show this in the contour plots of $W(X, P)$ in the phase space for two different values of ϕ for the lowest energy state for two different vibronic couplings in Fig. 9. From Fig. 9a one can see the almost circular feature of the phase space Wigner function for the lower coupling strength. On the other hand for stronger coupling $\lambda = 2.0$, the Wigner function becomes elliptic (see Fig. 9b). At the conical intersection point, the splitting of the Wigner function over the phase space is just complete for $\lambda = 1.0$ as shown in Fig. 9c. For $\lambda = 2.0$, the splitting is totally complete with the separation between the split centers being much higher compared to the $\lambda = 1.0$ case as is evident from Fig. 9d. This feature corresponds to the spreading of the wavepacket over the lower diabatic surface for high λ value. The interference structures, although much attenuated, can be seen at the CI point for $\lambda = 2.0$ but not in the case of $\lambda = 1.0$. The near cancellation of the interference structures of the Wigner function in phase space at and near the CI point is already discussed.

Now all these variations in nonclassicality and entanglement calculated for the lowest energy state with changing torsion angle can be explained with the variation of the wavefunction coefficients in Eq. (2). For low values of the torsion angle ϕ starting from $\phi = 0°$, the coefficient corresponding to the vacuum state of the vibrational mode

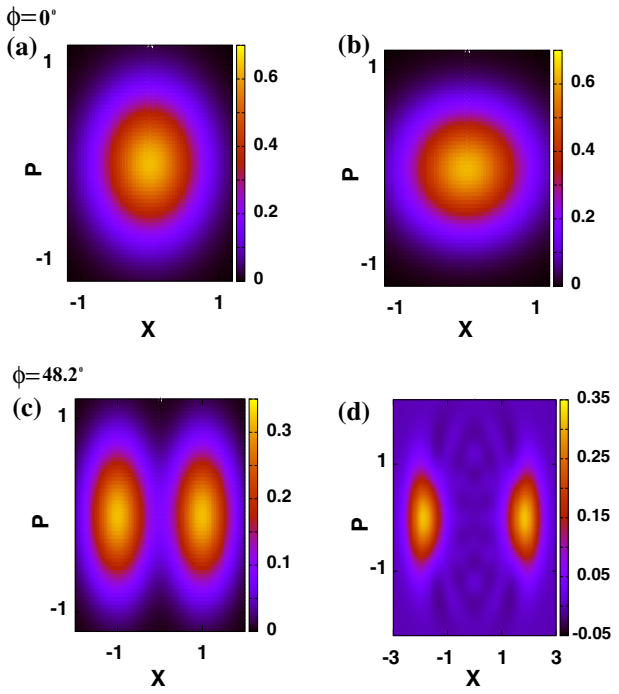

Fig. 9 Contour plots of the Wigner function $W(X, P)$ over the phase space of the vibrational motion for the lowest energy state with torsion angle $\phi = 0°$ and $\phi = 48.2°$. Two different vibronic coupling strengths are $\lambda = 1.0$ (**a**, **c**) and $\lambda = 2.0$ (**b**, **d**). X denotes the dimensionless normal coordinate of the vibration and P is its conjugate momentum

is important only *i.e.* $C^{j}_{1,0,0}$ for $j = 1$ is almost equal to 1.0. But as ϕ approaches the conical intersection point ($\phi = 48.2°$), coefficients with higher vibrational quantum number starts to become significant. This tendency is enhanced for stronger vibronic coupling λ. The mixing of these higher vibrational levels with the vacuum as a function of the torsion angle and the vibronic coupling enhances the nonclassical features and generates entanglement and squeezing in the composite states of the molecular system. The amount of entanglement and variances of the vibrational coordinate X and its conjugate momentum P measured for the lowest eigenstate, maximize at the conical intersection point.

Experimental detection of conical intersection in a molecule is very challenging as the energy gap of the molecule undergoes a drastic change over an ultrashort timescale, requiring a combination of extremely high temporal resolution and broad spectral tunability. Recent ultrafast transient optical spectroscopic experiments on molecular systems with *cis–trans* isomerization generated by torsional motion [46,47] detect interesting time-dependent optical signals like differential transmission signals. The theoretical model system used by us closely resembles these real molecular systems. The signals initially remain positive after the photoexcitation due to fluorescence/stimulated emission. The signals red shift rapidly and vanishes within few

hundred femtosecond depending on the nature of the system studied. After a very short passage through this spectroscopically 'dark' time window, there appears a photo-induced absorption signal that blue shifts rapidly to a steady value indicating the appearance of the molecule in the ground state and subsequent relaxation. For our case, the most important portion in the time-dependent ultrafast spectral analysis is the spectroscopically 'dark' time window as it is associated with the passage through a conical intersection [47]. As we characterize the conical intersection in terms of nonclassicality and quantum entanglement of the lowest energy state of the model system, we can say that the region of vanishing optical transition in these systems is connected with maximum entanglement.

5 Conclusion

We have investigated the effect of nonclassicality and quantum entanglement in a *cis–trans* isomerization reaction by treating the torsional coordinate parametrically for the understanding of the molecular system in presence of a conical intersection of the adiabatic potential energy surfaces. We have introduced a measure of entanglement in terms of the Wigner function matrices in the phase space of a vibrational mode which couples the two diabatic electronic states of the system and compared with other standard measures, namely, von Neumann entropy and partial transpose of joint density matrix. An interesting variation of nonclassicality and entanglement is found for the ground state as a function of the torsion angle and we have identified the conical intersection point of the two-dimensional adiabatic potential surfaces as the point of maximum quantum entanglement. The dip in the nonclassicality parameter, calculated as the volume of the negative portion of the Wigner function, at the CI point is explained as the cancellation of interference structures in the corresponding diagonal Wigner function matrix elements that conceals the highly nonclassical nature of the state. It is shown that the extent of nonclassical nature of the state as well as the entanglement strongly depends on the strength of the nonadiabatic vibronic coupling. This Wigner function measure of entanglement between electronic and vibrational degrees of freedom can be useful for systems with number of electronic states greater than two with a vibrational manifold where other methods are not directly applicable.

We have calculated the variances of the dimensionless normal coordinate and its conjugate momentum for the vibrational mode of the system and found interesting variations as a function of the torsion angle. Both the variances reach the maximum at the CI point. The uncertainty product also shows maximum deviation from the minimum uncertainty product value at the CI point depending on the vibronic coupling strength. There is also a significant amount of vibronic coupling dependent squeezing which is reflected in the contour plots of the Wigner function in phase space.

Experimental determination of conical intersection in molecular system is highly challenging. Recent ultrafast time-dependent optical spectroscopy experiments associate the spectroscopically 'dark' time window with the passage of the system through the conical intersection region. Here we characterize the conical intersection point as the point of maximum entanglement and connect the high entanglement region with vanishing spectral signal. Finally, our results suggest that one can control the entan-

glement between the vibrational and electronic subsystems by the manipulation of the molecular parameters such as torsion angle which can be prepared externally.

Acknowledgments K. B. acknowledges Dr. D. S. Kothari Fellowship, UGC, India for the partial financial support.

References

1. T.J. Dunn, I.A. Walmsley, S. Mukamel, Phys. Rev. Lett. **74**, 884 (1995)
2. U. Leonhardt, Phys. Rev. A **55**, 3164 (1997)
3. K.E. Cahill, R.J. Glauber, Phys. Rev. **177**, 1882 (1969)
4. S.M. Barnett, P.M. Radmore, *Methods in Theoretical Quantum Optics* (Clarendon Press, Oxford, 1997)
5. W.P. Schleich, Quantum Optics in Phase Space (Wiley, Berlin, 2001), and references therein
6. A. Kenfack, K. Zyczkowski, J. Opt. B Quantum Semiclassical Opt. **6**, 396 (2004)
7. J.P. Dahl, H. Mack, A. Wolf, W.P. Schleich, Phys. Rev. A **74**, 042323 (2006)
8. D.T. Smithey, M. Beck, M.G. Raymer, A. Faridani, Phys. Rev. Lett. **70**, 1244 (1993)
9. A.I. Lvovsky, H. Hansen, T. Aichele, O. Benson, J. Mlynek, S. Schiller, Phys. Rev. Lett. **87**, 050402 (2001)
10. A. Zavatta, S. Viciani, M. Bellini, Science **306**, 660 (2004)
11. A. Zavatta, V. Parigi, M. Bellini, Phys. Rev. A **75**, 052106 (2007)
12. A. Ourjoumtsev, R. Tualle-Brouri, P. Grangier, Phys. Rev. Lett. **96**, 213601 (2006)
13. A. Ourjoumtsev, A. Dantan, R. Tualle-Brouri, P. Grangier, Phys. Rev. Lett. **98**, 030502 (2007)
14. J. Janszky, A.V. Vinogradov, T. Kobayashi, Z. Kis, Phys. Rev. A **50**, 1777 (1994)
15. C. Kurtsiefer, T. Pfau, J. Mlynek, Nature **386**, 150 (1997)
16. H. Katsuki, H. Chiba, B. Girard, C. Meier, K. Ohmori, Science **311**, 1589 (2006)
17. S. Ghosh, U. Roy, C. Genes, D. Vitali, Phys. Rev. A **79**, 052104 (2009)
18. I.A. Walmsley, L. Waxer, J. Phys. B **31**, 1825 (1998)
19. C. Monroe, D.M. Meekhof, B.E. King, D.J. Wineland, Science **272**, 1131 (1996)
20. L.G. Lutterbach, L. Davidovich, Phys. Rev. Lett. **78**, 2547 (1997)
21. S. Wallentowitz, Filho R.L. de Matos, W. Vogel, Phys. Rev. A **56**, 1205 (1997)
22. S. Wallentowitz, Filho R.L. de Matos, S.C. Gou, W. Vogel, Eur. Phys. J. D **6**, 397 (1999)
23. A.D. O'Connell, et al. Nature **464**, 697 (2010)
24. K. Banerjee, G. Gangopadhyay, J. Phys. B At. Mol. Opt. Phys. **45**, 045102 (2012)
25. K. Banerjee, G. Gangopadhyay, J. Math. Chem. **51**, 2731 (2013)
26. G. Herzberg, H.C. Longuet-Higgins, Discuss. Faraday. Soc. **35**, 77 (1963)
27. H. Köppel, W. Domcke, L.S. Cederbaum, Adv. Chem. Phys. **57**, 59 (1984)
28. D.R. Yarkony, Rev. Mod. Phys. **68**, 985 (1996)
29. U. Manthe, H. Köppel, J. Chem. Phys. **93**, 345 (1990)
30. U. Manthe, H. Köppel, J. Chem. Phys. **93**, 1658 (1990)
31. L. Seidner, W. Domcke, Chem. Phys. **186**, 27 (1994)
32. W. Domcke, G. Stock, in *Advances in Chemical Physics, vol. 100* pp. 1–169 (1997)
33. M. Baer, G.D. Billing (eds.) The role of degenerate states in chemistry. In *Advances in Chemical Physics, vol. 124* (Hoboken, NJ, Wiley, 2002)
34. W. Domcke, D.R. Yarkony, H. Köppel (eds.), *Conical Intersections: Electronic Structure, Dynamics and Spectroscopy* (World Sci, Singapore, 2004)
35. B.G. Levine, T.J. Martinez, Annu. Rev. Phys. Chem. **58**, 613 (2007)
36. S. Parker, S. Bose, M.B. Plenio, Phys. Rev. A **61**, 032305 (2000)
37. S. Stenholm, K. Suominen, *Quantum Approach to Informatics* (Wiley, New York, 2005)
38. M. Horodecki, P. Horodecki, R. Horodecki, Phys. Lett. A **223**, 1 (1996)
39. A. Peres, Phys. Rev. Lett. **77**, 1413 (1996)
40. J. Liu, Z. Jiang, B. Shao, Phys. Rev. B **79**, 115323 (2009)
41. C.A. Vera, M.N. Quesada, H. Vinck-Posada, B.A. Rodriguez, J. Phys. Condens. Matter. **21**, 395603 (2009)
42. E. Schrödinger, Naturwissenschaften **23**, 807 (1935)
43. C. Gerry, P.L. Knight, Am. J. Phys. **65**, 964 (1997)

44. P.L. Knight, in *Quantum Fluctuations, Les Houches Session LXIII*, eds. S. Reynaud, E. Giacobino, J. Zinn-Justin (Elsevier, 1997) p. 41
45. M.V. Fedorov, M.A. Efremov, A.E. Kazakov, K.W. Chan, C.K. Law, J.H. Eberly, Phys. Rev. A **72**, 032110 (2005)
46. D. Polli, P. Altoe, O. Weingart, K. Spillane, C. Manzoni, D. Brida, G. Tomasello, G. Orlandi, P. Kukura, R.A. Mathies, M. Garavelli, G. Cerullo, Nature **467**, 440 (2010)
47. J. Briand, O. Bram, J. Rehault, J. Leonard, A. Cannizzo, M. Chergui, V. Zanirato, M. Olivucci, J. Helbingc, S. Haacke, Phys. Chem. Chem. Phys. **12**, 3178 (2010)